

Author's Proof

Carefully read the entire proof and mark all corrections in the appropriate place, using the Adobe Reader commenting tools ([Adobe Help](#)). Do not forget to reply to the queries.

We do not accept corrections in the form of edited manuscripts.

In order to ensure the timely publication of your article, please submit the corrections within 48 hours.

If you have any questions, please contact neuroscience.production.office@frontiersin.org.

Author Queries Form

Query No.	Details required	Author's Response
Q1	The citation and surnames of all of the authors have been highlighted. Please check all of the names carefully and indicate if any are incorrect. Please note that this may affect the indexing of your article in repositories such as PubMed.	
Q2	Confirm that the email address in your correspondence section is accurate.	
Q3	If you decide to use previously published, copyrighted figures in your article, please keep in mind that it is your responsibility, as the author, to obtain the appropriate permissions and licenses and to follow any citation instructions requested by third-party rights holders. If obtaining the reproduction rights involves the payment of a fee, these charges are to be paid by the authors.	
Q4	Ensure that all the figures, tables and captions are correct.	
Q5	Verify that all the equations and special characters are displayed correctly.	
Q6	Ensure, if it applies to your study, the ethics statement is included in the article.	
Q7	Ensure to add all grant numbers and funding information, as after publication this is no longer possible.	
Q8	Kindly confirm whether the Article title is correct.	
Q9	Kindly confirm whether the Affiliations are correct.	
Q10	Kindly provide expansion for the organization name "CIMEC" in "Affiliation 2" if applicable.	
Q11	Kindly provide expansion for the organization name "APSS" in "Affiliation 3" if applicable.	
Q12	Please include the following references in the reference list. Hackett, 2011; Jbabdi and Johansen-Berg, 2011; Tournier et al., 2011; Tardif and Clarke, 2011; Kawasaki et al., 2017.	
Q13	Please reduce short "running title" to maximum of five words.	

Query No.	Details required	Author's Response
Q14	We have moved the web links appearing inside the text as footnote. Please confirm if this is fine.	
Q15	<p>We have changed the following references inside the text as per the reference list. Kindly confirm if this is fine.</p> <p>“Aydogan et al., 2016” as “Aydogan and Shi, 2016”</p> <p>“Burton et al., 1976” as “Burton and Jones, 1976”</p> <p>“Dejerine, 1895” as “Dejerine and Dejerine-Klumpke, 1895”</p> <p>“Morel et al., 1992” as “Morel and Kaas”</p> <p>“Rheault et al., 2018” as “Rheault et al., 2019.”</p>	



A Missing Connection: A Review of the Macrostructural Anatomy and Tractography of the Acoustic Radiation

Chiara Maffei^{1,2*}, Silvio Sarubbo³ and Jorge Jovicich^{2,4}

¹ Harvard Medical School, Athinoula A. Martinos Center for Biomedical Imaging, Massachusetts General Hospital, Charlestown, MA, United States, ² Center for Mind/Brain Sciences - CIMeC, University of Trento, Trento, Italy, ³ Division of Neurosurgery, Structural and Functional Connectivity Lab Project, S. Chiara Hospital, Trento APSS, Trento, Italy, ⁴ Department of Psychology and Cognitive Sciences, University of Trento, Trento, Italy

OPEN ACCESS

Edited by:

Ricardo Insausti,
University of Castilla La Mancha,
Spain

Reviewed by:

David Reser,
Monash University, Australia
Hisayuki Ojima,
Tokyo Medical and Dental University,
Japan

*Correspondence:

Chiara Maffei
chiara.maffei@unitn.it

Received: 04 April 2018

Accepted: 15 February 2019

Published: xx February 2019

Citation:

Maffei C, Sarubbo S and Jovicich J (2019) A Missing Connection: A Review of the Macrostructural Anatomy and Tractography of the Acoustic Radiation. *Front. Neuroanat.* 13:27. doi: 10.3389/fnana.2019.00027

The auditory system of mammals is dedicated to encoding, elaborating and transporting acoustic information from the auditory nerve to the auditory cortex. The acoustic radiation (AR) constitutes the thalamo-cortical projection of this system, conveying the auditory signals from the medial geniculate nucleus (MGN) of the thalamus to the transverse temporal gyrus on the superior temporal lobe. While representing one of the major sensory pathways of the primate brain, the currently available anatomical information of this white matter bundle is quite limited in humans, thus constituting a notable omission in clinical and general studies on auditory processing and language perception. Tracing procedures in humans have restricted applications, and the *in vivo* reconstruction of this bundle using diffusion tractography techniques remains challenging. Hence, a more accurate and reliable reconstruction of the AR is necessary for understanding the neurobiological substrates supporting audition and language processing mechanisms in both health and disease. This review aims to unite available information on the macroscopic anatomy and topography of the AR in humans and non-human primates. Particular attention is brought to the anatomical characteristics that make this bundle difficult to reconstruct using non-invasive techniques, such as diffusion-based tractography. Open questions in the field and possible future research directions are discussed.

Keywords: acoustic radiation, auditory system, sensory pathways, auditory pathways, auditory tract, diffusion-based tractography

Abbreviations: AC, auditory cortex; AR, acoustic radiation; CC, corpus callosum; CR, corona radiata; CSD, constrained spherical deconvolution; dMRI, diffusion magnetic resonance imaging; DWI, diffusion weighted imaging; EC, external capsule; EEG, electroencephalography; FA, fractional anisotropy; FS, sylvian fissure; HC, healthy controls; HG, Heschl's gyrus; IC, inferior colliculus; IC, internal capsule; ICPL, posterior limb of the internal capsule; ICSL, sub-lenticular part of the internal capsule; ILE, inferior longitudinal fasciculus; LGN, lateral geniculate nucleus; MEG, magnetoencephalography; MGN, medial geniculate nucleus; ODF, orientation distribution function; OR, optic radiation; ROI, region of interest; PAC, primary auditory cortex; SNR, signal-to-noise ratio; STG, superior temporal gyrus; STP, superior temporal plane; TH, thalamus; WM, white matter; XRT, X-ray therapy.

INTRODUCTION

The acoustic radiation (AR) represents a highly-myelinated group of axonal projections and constitutes one of the primary sensory pathways of the primate brain, carrying auditory information from the thalamus to the cortex. The connectivity pattern of these fibers has been described in some detail in cytoarchitectonic and myeloarchitectonic studies of non-human primates (Polyak, 1932; Mesulam and Pandya, 1973; Morel et al., 1993; Hackett et al., 1998) and, at a more macroscopic level, in a few histological studies in humans (Flechsig, 1920; Pfeifer, 1920; Rademacher et al., 2002; Bürgel et al., 2006). However, the information obtained from non-human primate studies cannot be transferred directly to the human brain. Furthermore, such studies have focused mostly on the cytoarchitectonic aspects of the auditory cortices and their intrinsic connectivity, with little emphasis on the anatomical course of the AR itself. In humans, tracing studies are impossible *in vivo* and have restricted applications in post-mortem brains (Mesulam, 1979; Tardif and Clarke, 2001), while limited information can be drawn from old myeloarchitectonic post-mortem studies.

The advent of diffusion magnetic resonance imaging (dMRI) (Basser et al., 1994) and tractography (Mori et al., 1999) has made it possible to investigate the anatomy of the major white matter (WM) bundles of the human brain *in vivo* and non-invasively (Catani et al., 2002; Catani and de Schotten, 2008; Lawes et al., 2008). However, the AR constitutes a notable exception in this sense. This primary sensory bundle is largely absent from most tractography studies investigating audition and language and from human WM atlases (Thiebaut de Schotten et al., 2011). This is mainly due to the intrinsic anatomical characteristics of these fibers, which go beyond the current limits of dMRI tractography methods (Behrens et al., 2007; Jones and Cercignani, 2010; Daducci et al., 2016). Therefore, the diffusion-based tractography reconstruction of the AR remains highly challenging at present, discouraging its *in vivo* anatomical investigation in humans.

However, overcoming or circumventing these methodological considerations is essential, as successful *in vivo* reconstruction of the human auditory tract is of great importance for both clinical applications (e.g., pre-surgical mapping) and basic neurobiological research. Reliably revealing the 3D characteristics of this tract would help in correlating the anatomical and functional aspects of audition and in the study of human-only cognitive functions, such as language, both in healthy and pathological conditions.

The main aim of this review is to emphasize the paramount need for characterizing the human AR in both clinical and scientific contexts, which has yet to be done for a number of reasons that we discuss. This review collates the available information from primate studies on the anatomy, topography, and course of the AR, with particular emphasis on the anatomical features that make this tract extremely challenging to study, even for state-of-the-art dMRI tractography techniques. Additionally, recent attempts to reconstruct the AR using diffusion-based tractography methods will be discussed. Finally, open questions in the field will be presented and possible future research directions considered.

THE ACOUSTIC RADIATION IN PRIMATES

The auditory system of mammals is a complex network of parallel and overlapping axonal projections that connect subcortical nuclei and cortical regions. It encodes and transmits stimuli coming from the acoustic environment, enabling an organism to detect a sound in its environment, determine the direction from which it originated, discriminate among potential sources, and thereby, react or communicate with conspecifics. **Figure 1** provides a schematic representation of the human ascending auditory system and its sub-cortical relays, as it is commonly described in both the scientific literature and neuroanatomy textbooks (Moller, 2006; Brugge, 2013). The thalamo-cortical projections of this system, which connects the medial geniculate nucleus (MGN) to auditory cortex, constitute the AR (**Figure 1**).

Anatomical knowledge of the human AR mainly comes from pioneering investigations at the beginning of the 20th century (Dejerine and Dejerine-Klumpke, 1895; Flechsig, 1920; Pfeifer, 1920). Since these early studies, very limited additional information on this structure has been reported for humans (Rademacher et al., 2001, 2002; Bürgel et al., 2006). Most of the anatomical and functional organization of the mammalian auditory system has been inferred from animal studies, mainly non-human primates and cats (Morel and Kaas, 1992; Hashikawa et al., 1995; Hackett et al., 1998; Kaas and Hackett, 2000; Hackett et al., 2001; Jones, 2003; de la Mothe et al., 2006; Lee and Winer, 2008). However, these studies primarily focus on the topographical mapping between the thalamus and auditory cortex without documenting the spatial connection pattern and course of these fibers (Jones, 2003; Hackett, 2011). As a consequence, most neuroanatomical books only report schematic drawings of this pathway (e.g., **Figure 1**). Furthermore, although comparative studies have shown similar features across human and non-human primate brains, cortical and subcortical architectonic differences, as well as cognitive dissimilarities,

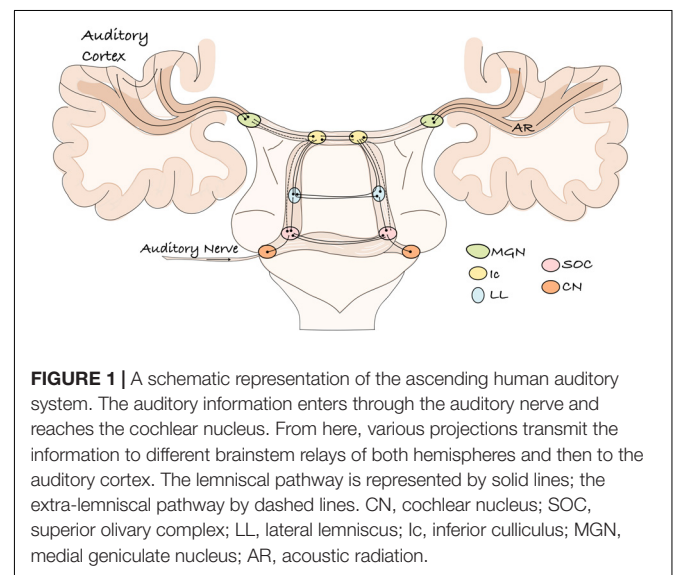


FIGURE 1 | A schematic representation of the ascending human auditory system. The auditory information enters through the auditory nerve and reaches the cochlear nucleus. From here, various projections transmit the information to different brainstem relays of both hemispheres and then to the auditory cortex. The lemniscal pathway is represented by solid lines; the extra-lemniscal pathway by dashed lines. CN, cochlear nucleus; SOC, superior olivary complex; LL, lateral lemniscus; IC, inferior colliculus; MGN, medial geniculate nucleus; AR, acoustic radiation.

229 exist (Galaburda and Sanides, 1980; Galaburda and Pandya, 286
 230 1983; Schmahmann et al., 2007; Passingham, 2009; Thiebaut 287
 231 de Schotten et al., 2012). Thus, it is important to understand 288
 232 the commonalities among primate species and to identify 289
 233 potentially unique aspects of the human auditory system that 290
 234 might be related to our ability to perceive and process language- 291
 235 specific stimuli. *In vivo* diffusion imaging techniques constitute a 292
 236 powerful tool in investigating these topics. 293

237 In the next section, we briefly review the AR microstructural 294
 238 topography, as described in animal studies, and its 295
 239 macrostructural anatomy, which has been gleaned from 296
 240 human research. Our goal is to provide a more complete 297
 241 anatomical profile of this bundle across species and to highlight 298
 242 the existing gap of topographical information between invasive 299
 243 and non-invasive studies. In particular, we focus on the AR 300
 244 *in vivo* imaging literature, reviewing recent attempts to visualize 301
 245 this tract using tractography techniques. 302

246 247 248 249 The Acoustic Radiation in Invasive Studies

250 The axonal connections between the thalamus and the auditory 303
 251 cortex have been investigated in animals using different invasive 304
 252 techniques. These fibers stem from the medial geniculate nucleus 305
 253 of the thalamus (MGN), as first described by von Monakow 306
 254 (1882), and contact a specific area on the posterior part of 307
 255 the Sylvian fissure (Minkowski, 1923; Polyak, 1932), which has 308
 256 been described as a “rudimentary transverse temporal gyrus” 309
 257 (Walker, 1937) in monkeys. In most species, three major divisions 310
 258 of the MGN are identified: ventral (or principal), dorsal (or 311
 259 posterior), and medial (or magnocellular) (Winer et al., 2001; 312
 260 Jones, 2003). Each of these divisions has unique connections 313
 261 to different cortical regions. The ventral division receives input 314
 262 from the central nucleus of the inferior colliculus (Ic) and 315
 263 almost exclusively projects to what is defined as the core region 316
 264 of the auditory cortex (Mesulam and Pandya, 1973; Burton 317
 265 and Jones, 1976; Morel and Kaas, 1992; Morel et al., 1993; 318
 266 Hashikawa et al., 1995; Rauschecker et al., 1997). This region 319
 267 is distinguished by dense immunoreactivity for the calcium- 320
 268 binding protein parvalbumin, as most of its inputs come from 321
 269 the ventral MGN parvalbumin immunoreactive cells (Molinari 322
 270 et al., 1995), even if some connections with the other MGN 323
 271 divisions appear to exist (Luethke et al., 1989; Morel et al., 324
 272 1993). This region occupies a portion of the caudal superior 325
 273 temporal plane (postero-medial part of the Heschl’s gyrus in 326
 274 humans) and it is characterized by a dense population of small 327
 275 granule cells (e.g., koniocortex) with a well-developed layer IV 328
 276 (Merzenich and Brugge, 1973; Seldon, 1981). Both the ventral 329
 277 MGN and the core region show a tonotopical organization in 330
 278 which the representation of frequencies is spatially organized. 331
 279 This suggests a topographical organization of fibers connecting 332
 280 similar frequency domains in these two structures (Burton and 333
 281 Jones, 1976; Molinari et al., 1995). The core region is surrounded 334
 282 by a secondary narrow belt region and a third, more lateral region 335
 283 that occupies the lateral surface of the superior temporal gyrus 336
 284 (Hackett et al., 1998; Kaas and Hackett, 2000). This latter “para- 337
 285 belt” region is generally considered to be a higher-order auditory 338

286 region or auditory association cortex that integrates auditory 287
 288 with non-auditory multisensory information (Hackett et al., 289
 290 1998). These regions are less responsive to pure tone sounds, 291
 292 preferring more complex sounds, and do not show the clear 293
 294 tonotopical organization typical of the core region (Rauschecker 295
 296 et al., 1995; Jones, 2003). The dorsal and medial divisions of the 297
 298 MGN constitute the major inputs to these secondary auditory 299
 299 association regions. These nuclei receive inputs from the external 300
 300 nucleus of the Ic, as well as from lower brainstem relays, and 301
 301 bypass the core region to project to secondary auditory and 302
 302 other cortical regions (Rauschecker et al., 1997; Jones, 2003; 303
 303 Winer and Lee, 2007). 304

298 Projections from the ventral MGN to the core region 299
 299 correspond to the most direct classic auditory pathway, also 300
 300 called the lemniscal pathway. These parallel connections are 301
 301 tonotopically organized and their neurons show sharp responses 302
 302 to tones (Morel et al., 1993). Direct projections from the other 303
 303 MGN divisions to secondary auditory cortical regions are part 304
 304 of the extralemniscal (or non-lemniscal) auditory pathway. 305
 305 These fibers are separate from but lie adjacent to those of 306
 306 the lemniscal pathway in the ascending auditory system. In 307
 307 addition, their subdivision continues at the cortical level, where 308
 308 the non-lemniscal pathway has stronger and more diffuse 309
 309 connections with regions surrounding the core region (Lee 310
 310 and Sherman, 2010). These pathways are less tonotopically 311
 311 organized and their neurons demonstrate fewer sharp 312
 312 responses to sounds. 313

313 Classical studies in non-human primates focus on the 314
 314 topography of the connectivity between the MGN and the 315
 315 auditory projection cortical territory but provide no information 316
 316 on either the course and extension of the AR tract itself or 317
 317 its relationship with the other WM pathways of the brain. 318
 318 Using Marchi axonal degeneration, Polyak (1932) provided a 319
 319 detailed description of the course of this tract in rhesus macaques 320
 320 (**Figure 2**). He describes a dense bundle of closely assembled 321
 321 fibers that leaves the MGN, turns laterally and crosses the most 322
 322 ventral portion of the internal capsule (IC) immediately above 323
 323 the lateral geniculate nucleus (LGN) of the thalamus (**Figure 2**). 324
 324 At this level, these fibers are distinguishable from somato- 325
 325 sensory fibers because of their nearly horizontal orientation. 326
 326 The AR then bends ventrally and reaches the external capsule 327
 327 (EC) by passing through the ventral edge of the posterior 328
 328 putamen. Once there it meets other projection and association 329
 329 bundles before finally reaching the WM of the superior temporal 330
 330 convolution close to the Sylvian fissure (**Figure 2**). He describes 331
 331 the AR as a regularly arranged projection system, where fibers 332
 332 lie parallel to one another until gradually diverging only when 333
 333 approaching the cortex. 334

334 Classical topographical descriptions in humans (**Figure 3**) 335
 335 provide a very similar description (Dejerine and Dejerine- 336
 336 Klumpke, 1895; Flechsig, 1920; Pfeifer, 1920) of the AR, which 337
 337 may be summarized as follows. The AR leaves the MGN and 338
 338 travels in an antero-lateral direction; it then passes through the 339
 339 posterior portion of the IC, proceeds along the corona radiata 340
 340 and curves around the inferior portion of the circular sulcus 341
 341 of the insula before entering the transverse temporal gyrus 342
 342 of Heschl (HG) in a ventral-to-dorsal direction (Pfeifer, 1920).

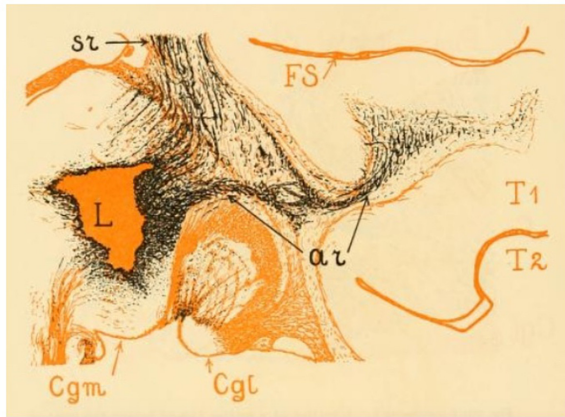


FIGURE 2 | The image shows the acoustic radiation fibers in the rhesus monkey. The lesion (L) was located in the posterior thalamus. From here we can see numerous thalamocortical (or somato sensory) (sr) and auditory (ar) fibers emerging. The tsr and ar fibers form a system of which the ar occupies the most ventral position. The acoustic radiation occupies the upper half of the white matter of the superior temporal convolution (T1) and enters the cortex of the lower wall of the Sylvian fissure (FS). The level of this figure is immediately behind the posterior extremity of the lentiform nucleus; the entire length of the acoustic radiation is visible here. Cgm, medial geniculate nucleus; Cgl, lateral geniculate nucleus (adapted from Polyak, 1932; <https://archive.org>, public domain).

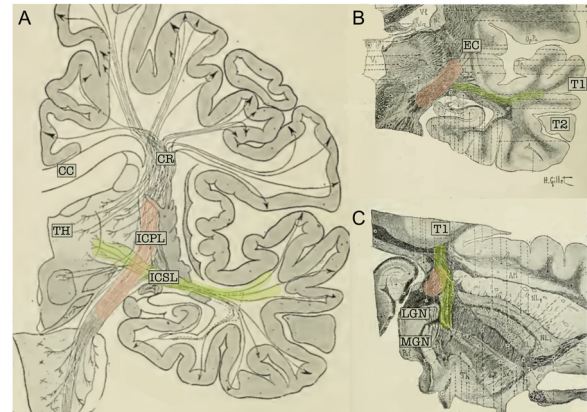


FIGURE 3 | (A) Schematic representation of the projection fibers of the human brain (coronal view). (B) Coronal cut through the middle section of the thalamus. (C) Axial section of the brain; cut through the inferior thalamus. In the three panels, fibers belonging to the acoustic radiation have been highlighted in green and fibers of the internal capsule in pink. The acoustic radiation projects from the thalamus (TH) to the first temporal circonvolution (T1) and passes through the sub-lenticular and posterior segment of the internal capsule. This map clearly highlights the crossing between these two fiber systems. CC, Corpus callosum; EC, external capsule; ICPL, Posterior limb of the internal capsule; ICSSL, sub-lenticular part of the internal capsule; CR, corona radiata; LGN, lateral geniculate nucleus; MGN, medial geniculate nucleus; T1, first temporal circonvolution; TH, thalamus (adapted from Dejerine and Dejerine-Klumpke, 1895; <https://archive.org>, public domain).

At this macrostructural level, both animal and human studies delineate a bundle with a transverse orientation that lies adjacent to and crosses over other main WM bundles before reaching the auditory cortex. In both animals and humans, the AR intermingles with the fibers of the IC in its most posterior portion. Furthermore, Dejerine and Dejerine-Klumpke (1895) described the close proximity of the AR to the optic radiation (OR) at the stemming point in the thalamus, defining this region as the “*carrefour sensitive*” (sensory intersection). Polyak (1932) also studied this region, stating that the OR and AR, although lying close together, are completely separate: the AR is located more anterior and crosses at a right angle above the OR, which follows a posterior direction in the sagittal plane. As will be discussed in the following section, this configuration and certain other anatomical features of the AR pose serious challenges to its 3D tractography reconstruction.

The myeloarchitectonic maps from Dejerine and Dejerine-Klumpke (1895) and Flechsig (1920), while being of invaluable historical significance, cannot be used to extract precise anatomical information that can be applied to modern brain atlases or neuroimaging studies. More recently, radiological information about the AR anatomical organization was obtained in human post mortem myelin-stained sections (Rademacher et al., 2002; Bürgel et al., 2006). These studies confirm the classical topographical description of the acoustic fibers and are of great importance as they represent the main reference framework for *in vivo* imaging studies of this brain region and provide the opportunity to investigate inter-subject variability and hemispheric asymmetry. Previous studies have found that the AR does not enter the lenticular nucleus, but rather runs dorsally

to the OR, crossing the temporal isthmus as it ascends to the auditory cortex (Pfeifer, 1920; Polyak, 1932; Bürgel et al., 2006). Fanning of these fibers in HG creates a hat-like structure that covers the posterior end of the lenticular nucleus (Rademacher et al., 2002).

According to Flechsig (1920), these fibers are divisible into two bundles, one of which ascends near the Ec and enters the auditory cortex from the superior-posterior side. The other bundle courses for some distance in the company of the OR before passing behind and below the *fossa sylvii* where it pierces the bases of the middle and inferior temporal gyri to reach the transverse temporal gyrus or gyri. Similarly, early evidence from animal studies suggests that the AR is subdivided into dorsal and ventral components (von Monakow, 1882), although, Rademacher et al. (2002) found more recently only a single and heavily myelinated bundle.

Overall, the macrostructural description of the AR in humans resembles the description of this tract in non-human primates. The origin and termination of this bundle, together with the extension and relationship to other WM bundles, is maintained. However, the macro- and micro-anatomical correspondence between the different cortical regions in monkeys and humans is not straightforward (Baumann et al., 2013). Compared to non-human primates, the human cortical surface of the auditory regions demonstrates additional gyri and higher inter-subject and interhemispheric variability (Galaburda et al., 1978; Hackett et al., 2001), both of which may affect the AR anatomy. The human auditory cortex also shows higher differentiation into

457 sub-regions as compared to non-human primates, and the core
458 region is larger than the belt region (the opposite is true for
459 monkeys) (Fullerton and Pandya, 2007). Both the differences
460 in cortical anatomy between non-human primates and humans
461 and the major variability of cortical and subcortical structures
462 across subjects and hemispheres in humans (Bürgel et al., 2006)
463 raise interesting questions about the possibility of a relationship
464 between such morphological differences and human-only
465 language abilities.

466

467

468

469

The Acoustic Radiation in Non-invasive Tractography Studies

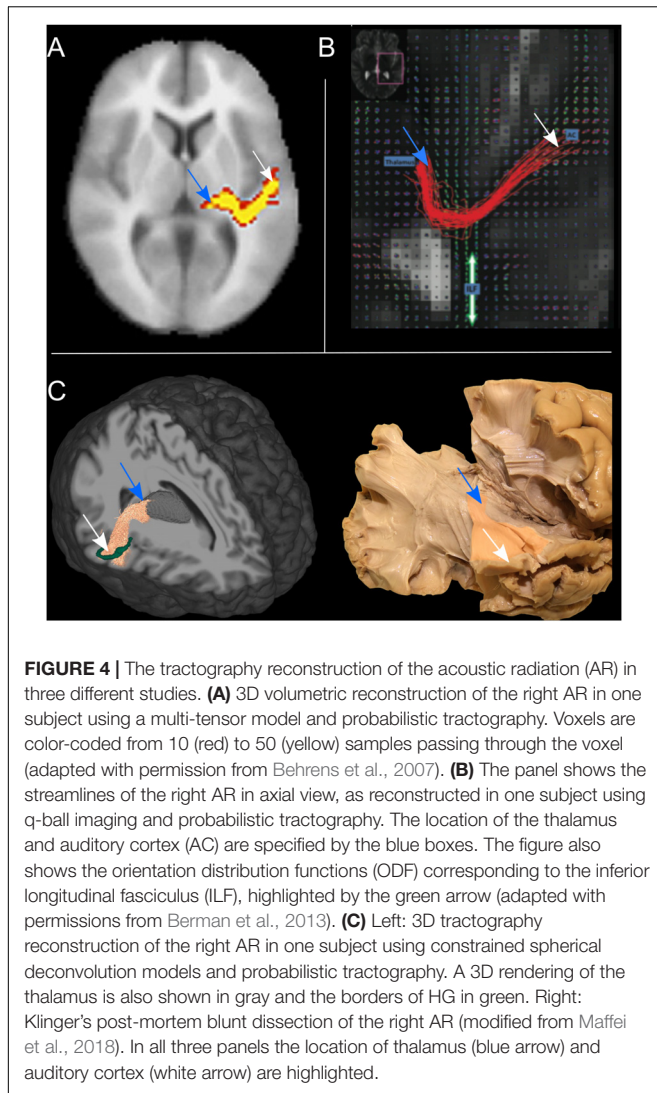
470 Diffusion MRI (dMRI) tractography allows for the investigation
471 of WM architecture in the human brain non-invasively
472 *in vivo*. Since its first applications (Mori et al., 1999), most
473 of the well-known WM bundles of the human brain have
474 been reconstructed using diffusion-based tractography methods
475 (Catani and Thiebaut de Schotten, 2008; Lawes et al., 2008).
476 Despite its potentials, dMRI tractography has several important
477 limitations that have been discussed in depth in the literature
478 (e.g., Jones and Cercignani, 2010; Thomas et al., 2014; Maier-
479 Hein et al., 2017). In principle, these limitations affect most
480 tractography reconstructions, but here we focus on how
481 they particularly affect the 3D reconstruction of the AR.
482 Reconstructing the AR three-dimensionally is highly challenging
483 at present due to the anatomical features described in the
484 previous sections: its relatively small size, transversal orientation,
485 and location in a region with a high density of crossing fibers.
486 This largely prevents the inclusion of this particular tract in most
487 tractography investigations.

488 As shown in the previous section (see **Figures 2, 3**), in its
489 medio-lateral course from the MGN to the HG, the AR lies
490 in a nearly horizontal position and, for this reason, crosses
491 some of the major fiber systems of the human brain: internal
492 capsule, external capsule, and posterior thalamic radiation
493 (Maffei et al., 2018). Resolving the fiber crossing is a well-
494 known challenge in dMRI (Tuch et al., 2002; Dell'Acqua and
495 Catani, 2012; Jeurissen et al., 2013). The classic tensor model
496 (Basser et al., 1994) is capable of characterizing only one
497 main fiber orientation per voxel and it has been shown to
498 constantly fail in regions where voxels contain complex fiber
499 architectures (Behrens et al., 2007; Jbabdi and Johansen-Berg,
500 2011). The impact of this limitation is particularly evident for
501 non-dominant tracts, given that the orientation produced by
502 the tensor will be closest to the largest contributing direction
503 in most cases. This effect is amplified at the low resolution
504 of commonly available diffusion protocols due to within-voxel
505 partial volume averaging effects (Tournier et al., 2011). When
506 implemented in tractography studies, the diffusion tensor model
507 has proven to be incapable of detecting the 3D profile of the AR.
508 Streamlines are either truncated when entering voxels containing
509 major inferior-superior orientations or erroneously embedded
510 in the reconstruction of these major projection bundles, with
511 no visible streamlines contacting the HG (Behrens et al., 2007;
512 Crippa et al., 2010; Berman et al., 2013). This has likely
513 been the primary factor preventing the investigation of the

auditory system by means of diffusion-based tractography. Some
studies have used the diffusion tensor to investigate the WM
microstructure of the auditory system, limiting the structural
investigation of the auditory pathways to the extraction of mean
quantitative diffusion measures [e.g., fractional anisotropy (FA)]
from specific regions of interest (ROI) (Chang et al., 2004; Lee
et al., 2007; Lin et al., 2008; Wu et al., 2009). However ROI-
based analysis can lead to inaccurate results, especially for WM
tracts that are extremely variable across subjects, such as the AR
(Rademacher et al., 2002). Therefore, it is typically preferable
to map the exact anatomy of such WM tracts in individual
subjects/patients.

To address the intrinsic limitations of the tensor
formalization, more advanced models have been introduced
that can better account for fibers crossing, by modeling more
than one fiber population per voxel (Tuch, 2004; Tournier
et al., 2008; Descoteaux et al., 2009). These models open up the
possibility of propagating streamlines through crossing fiber
regions, thus allowing the reconstruction of non-dominant WM
bundles, such as the AR. However, together with the low-level
diffusion model employed, other parameters play a role in the
accurate reconstruction of WM bundles, such as the tractography
parameters chosen and the strategy to define inclusion ROIs.
Here we report studies that reconstruct the AR 3D tractography
profile *in vivo* using multi-fiber-based models (**Figure 4**), taking
into consideration the different combinations of acquisition
parameters, diffusion models and ROIs selection strategies that
they used (**Table 1**).

Behrens et al. (2007) were able to visualize the course of the AR
from the MGN to the cortex using the ball-and-stick model and
probabilistic tractography (Behrens et al., 2003) (**Figure 4A**). The
authors demonstrate how this multi-fiber model can reconstruct
the AR, overcoming the limitations of the tensor model. Three
following studies were then able to demonstrate the reliability of
this model for successful *in vivo* reconstruction of the profile of
the auditory tract in both healthy subjects and those with tinnitus
(Crippa et al., 2010; Javad et al., 2014; Profant et al., 2014). In these
studies, different combinations of inclusion ROIs were used to
isolate the AR, including the Ic, the MGN, and both functionally
and manually defined HG. Nevertheless, the profile of the 3D
tractography reconstruction looks visually similar across the four
studies and shows connections between the posterior thalamus
and the auditory region WM. However, artifacts are visible
along the inferior-superior axis in the middle part of the AR
at the level of the crossing with the IC and these false positive
reconstructions are likely to be related to the probabilistic nature
of the diffusion model and tractography algorithm used. Despite
the inclusion of false positive signals in the reconstructions,
the ball-and-stick model has the important advantage of being
accessible to low *b*-value ($b = 1000 \text{ s/mm}^2$) diffusion protocols
which makes it suitable for clinical investigations of the AR.
Berman et al. (2013) (**Figure 4B**) used a solid-angle q-ball model
(Aganj et al., 2010) and probabilistic tractography to successfully
reconstruct the auditory connections between the MGN and
HG. This reconstruction looks anatomically very accurate and
free of false positive artifacts. However, q-ball methods require
higher *b*-value diffusion data ($b \geq 3000 \text{ s/mm}^2$). In these models,



the angular resolution of the reconstructed diffusion profiles is increased and the crossing fiber configurations are correctly represented (Tournier et al., 2013), although they pose limitations to its use in clinical populations. Our group (Maffei et al., 2018) used ultra-high b -value Human Connectome Project diffusion data-sets (Fan et al., 2015) and spherical deconvolution (Tournier et al., 2008) to reconstruct AR streamlines using probabilistic tractography. We compared the results to Klinger's post-mortem blunt micro-dissections (Figure 4C), a method based on a brain freezing technique optimized to reveal WM (Ludwig and Klingler, 1956). This approach has been used in several studies to evaluate tractography accuracy (Fernández-Miranda et al., 2015; De Benedictis et al., 2016; Pascalau et al., 2018). The obtained reconstructions agreed with the AR anatomy revealed in the post-mortem dissections and no additional exclusion regions were needed to isolate the AR profile. However, the ultra-high b -values used in this study ($b \leq 10,000$ s/mm²) are very rarely achievable, even in research settings. More recently, Yeh et al. (2018) published a population-averaged atlas

of several WM connections, including the AR, using q-space diffeomorphic reconstruction (QSDR) (Yeh and Tseng, 2011) and deterministic tractography for multiple fiber orientations. In their approach, the high angular and spatial resolution of the data (1.25 mm isotropic, and $b \leq 3000$ s/mm²) and the large sample (842 subjects) allowed them to reduce the rate of false positive artifacts. However, the AR profile shown in this study, while correctly originating at the posterior thalamus, does not reach the expected auditory cortex on the superior side of the temporal lobe.

Overall, the reconstructed 3D profiles shown in these studies are in accordance with the macrostructural landmarks defined by classic anatomical studies: streamlines originate in the posterior thalamus and course in an antero-lateral direction to terminate in the temporal lobe (Dejerine and Dejerine-Klumpke, 1895). However, AR reconstructions are still highly variable across studies. In particular, while showing similar profiles at the thalamic stemming region, reconstructions differ as they approach the cortex, either falling short of reaching the HG (Crippa et al., 2010; Yeh et al., 2018) or creating false positive artifacts at the intersection with vertically oriented fibers (Javad et al., 2014; Maffei et al., 2018). Moreover, disagreement about the relationship with neighboring tracts exists. Berman et al. (2013) suggest that AR streamlines cross the inferior longitudinal fasciculus (ILF), while Behrens et al. (2007) and Javad et al. (2014) claim that they cross the OR. In a recent work from our group, we did not find that the AR is in close proximity to the ILF (Maffei et al., 2018), supporting older studies that report no crossing between the AR and OR (Pfeifer, 1920; Polyak, 1932), as described above. In addition to variability across studies, low reproducibility across subjects is also reported. Some groups have been able to reconstruct AR tracts on both hemispheres on 100% of subjects (Behrens et al., 2007; Profant et al., 2014; Maffei et al., 2017). In contrast, even when using similar diffusion models (e.g., ball-and-stick), other studies report reconstructions successful in both hemispheres in much lower proportions, such as 35–50% (Crippa et al., 2010) or 71–86% (Javad et al., 2014).

We suggest that the present variability and low reproducibility in the reconstructed AR profile are related to a combination of some of the specific characteristics of the AR that make its tractographic reconstruction quite challenging, even for state of the art tractography techniques: its anatomical location, small size, and inter-individual anatomical variability.

As alluded to in the previous section, the AR constitutes a compact but relatively short and small bundle that lies horizontally in a region with a high density of vertical fibers. Even if multi-fiber models proved capable of representing this crossing, the degree to which this crossing can be accurately resolved in the final 3D reconstruction also depends on the tractography algorithm used and the intrinsic angular resolution of the dMRI data (Tournier et al., 2013). For example, using a higher b -value (Berman et al., 2013; Maffei et al., 2018) might help improve accuracy of results relative to those obtained with lower b -value data (Crippa et al., 2010). However, in these studies several exclusion ROI have been employed to either constrain tractography (Behrens et al., 2007) or clean the results (Crippa et al., 2010). This renders the accuracy of

TABLE 1 | The table reports the main acquisition and tractography parameters used to reconstruct the AR in the listed studies.

References	Diffusion MRI acquisition parameters	Diffusion model	Inclusion ROIs	Exclusion ROIs	Group size	Success rate
Behrens et al., 2007	60 DWI directions B = 1000 s/mm ² 2 × 2 × 2 mm	Ball and stick	MGN (Manual) HG (Single slice)	Other thalamic fibers	9 (HC)	100%
Crippa et al., 2010	60 DWI directions B = 800 s/mm ² 1.8 × 1.8 × 2 mm	Ball and stick	Ic (Manual) HG (Manual)	Motor fibers	25 (15 HC, 10 tinnitus)	35–50%
Berman et al., 2013	64 DWI directions B = 3000 s/mm ² 2 × 2 × 2 mm	Solid angle q-ball	MGN (Manual) HG (Freesurfer)	Putamen, CC, CG, Pallidum	25 (HC)	98%
Javad et al., 2014	64 DWI directions B = 1400 s/mm ² 2.3 × 2.3 × 2.3 mm	Ball and stick	MGN (Manual) HG (fMRI)	Not applied	14 (HC)	71–86%
Profant et al., 2014	64 DWI directions B = 1100 s/mm ² 2 × 2 × 2 mm	Ball and stick	Ic (Manual) HG-WM (Freesurfer)	Rostral thalamus, sagittal slice + manual	54 (20 HC, 34 hearing deficit)	100%
Maffei et al., 2018	576 DWI directions B = 1000, 3000, 5000, 10,000 s/mm ² 1.5 × 1.5 × 1.5 mm	CSD	TH (FSL) HG (Manual)	Not applied	4 (HC)	100%
Yeh et al., 2018	90 DWI directions B = 1000, 2000, 3000 s/mm ² 1.25 × 1.25 × 1.25 mm	QSDR	Clustering + manual labeling	/	842 (HC)	/

The acquisition parameters column provides the number of diffusion encoding directions, the b-factor (s/mm²), and the spatial resolution (mm). The inclusion ROIs column indicates whether seed and target regions were selected manually or with other methods. Some tractography studies performed reconstructions in both directions and results were summed. The success rate column reports the percentage of subjects showing successful AR tractography reconstructions in both hemispheres. DWI, diffusion MRI encoding directions; CG, Cingulate Gyrus; CSD, Constrained Spherical Deconvolution; HG, Heschl's Gyrus (gray and white matter); HG-WM, Heschl's Gyrus (only white matter); Ic, Inferior Culliculus; MGN, Medial Geniculate Nucleus; QSDR, q-space diffeomorphic reconstruction; TH, Thalamus; HC, healthy controls.

the final reconstructions sensitive to the selection of these ROI, complicating comparisons across studies.

The use of different ROI selection strategies can strongly affect the resulting tractography reconstructions. The HG is a complex structure that shows large variability in sulcal landmarks across subjects and hemispheres (Rademacher et al., 2001), whereas the MGN is a very small structure, varying from 74 to 183 mm³ (Kitajima et al., 2015), making it difficult to locate in neuroimaging data and also highly variable across individuals and hemispheres (Rademacher et al., 2002). Therefore, this variability poses difficulties in the selection of the ROIs used to initiate the tractography reconstruction or to perform the virtual dissections. For example, while reliable automatic segmentation tools for the entire thalamus are available in different public software packages (e.g., FSL¹, Freesurfer²), it is far more challenging to automatically segment smaller structures, such as the MGN, due to both their size and their lower MRI contrast with neighboring WM. Alternative solutions exist but are also challenging. For example, subject-specific manual segmentations of MGN can lead to high anatomical accuracy, but they are very time intensive and, therefore, costly to do in large subject cohorts. Brain atlases also can be used to define the MGN, however

given the small size and inter-subject variability, atlas-driven segmentations are unlikely to provide a good anatomical match for all subjects. The development of more accurate automatic parcellation techniques for the thalamic nuclei is expected to improve the accuracy of seed-to-target definition and, thus, of the resulting tractography reconstructions. Recently, a new and promising probabilistic atlas of the thalamic nuclei has been proposed based on a combination of *ex vivo* MRI and histology (Iglesias et al., 2018).

Future research in the field should focus on how to improve the sensitivity and reproducibility of the tractography reconstruction of this bundle. This could be achieved by inputting prior anatomical knowledge in the tractography process, as it is implemented in global-tractography-based frameworks (Yendiki et al., 2011) or more recently developed bundle-specific algorithms (Rheault et al., 2019). Parallel to these advances at the tractography level, there have been efforts in validating tractography results at a micro-anatomical scale. As this validation process progresses, we expect to expand our knowledge of the exact boundaries of the human AR and, consequently, better inform its tractography reconstruction and improve accuracy of tractography results. A more accurate tractography investigation of the AR could expand our structural and functional knowledge of the auditory system, as proposed in the next section.

¹<https://fsl.fmrib.ox.ac.uk/fsl/>

²<http://surfer.nmr.mgh.harvard.edu/>

799 THE ACOUSTIC RADIATION: 800 FUNCTIONAL AND CLINICAL 801 IMPLICATIONS 802

803 The reliable *in vivo* reconstruction of the AR in humans may
804 help the exploration of the neuro-anatomical and functional
805 mechanisms underlying auditory processing and language
806 comprehension. The precise characterization of the AR can
807 provide information useful for clinical applications, such as
808 in diagnosis and treatment of hearing and speech disorders,
809 recovery from injury, and performance of interventions that
810 can damage the AR, such as brain surgery or radiation
811 treatments. This section provides a brief review of basic and
812 clinical research areas that could benefit from an improved
813 characterization of the AR.
814

815 Language and Auditory Perception

816 The ability to communicate through speech is quintessentially
817 human. However, the anatomical organization and the functional
818 mechanisms underlying speech comprehension in the brain are
819 still not understood completely. The acoustic information that
820 reaches the primary auditory cortex via the AR fibers is processed
821 within neural networks that depend on cortico-cortical short-
822 and long-range connections involving temporal, parietal and
823 frontal regions, as schematized in the dual-stream model (Hickok
824 and Poeppel, 2007; Saur et al., 2008; Friederici, 2009). Within
825 this processing network, it is unclear where language-specific
826 processing starts and whether the auditory cortex is involved
827 in speech-specific analysis. Some theories suggest that the left
828 auditory cortex is specialized in processing temporal cues that
829 are fundamental for speech comprehension (Zatorre et al., 2002;
830 Poeppel, 2003) and that this language-specific encoding might
831 actually start at the subcortical level (Hornickel et al., 2009). The
832 diffusion-based reconstruction of the AR, and of the auditory
833 pathways at large, could help address the structural-functional
834 relationship of speech perception. At the structural level, it would
835 be interesting to understand whether the AR exhibits a degree of
836 leftward lateralization in its volume, as demonstrated for some of
837 the other WM bundles implicated in language processing (Catani
838 et al., 2007). Reports on the macroscopic volumetric asymmetry
839 of cortical auditory regions have been known for some time (Von
840 Economo and Horn, 1930; Galaburda et al., 1978; Geschwind
841 and Galaburda, 1985; Penhune et al., 1996), but only one study
842 specifically investigated the hemispheric lateralization of the AR
843 (Bürgel et al., 2006). At the functional level, the recent association
844 of tractography and neurophysiological techniques [such as
845 magnetoencephalography (MEG) and electroencephalography
846 (EEG)] opens interesting possibilities for investigating these
847 topics. EEG metrics have been recently correlated with diffusion
848 metrics in the investigation of the OR (Renauld et al.,
849 2016). Similarly, EEG/MEG- and tractography-derived measures
850 could be combined to investigate the relationship between
851 temporal cortical regions and auditory function in both healthy
852 subjects and patients.
853

854 On a finer scale, AR streamline terminations could be
855 combined with functional MRI to provide critical insights into

the subdivision of the auditory cortex, the borders of which are
still not clearly defined using *in vivo* neuroimaging methods
(Baumann et al., 2013). In this sense tractography could be
used to investigate the topographical organization of the AR
with respect to the different subdivisions of the auditory cortex.
The different auditory cortical regions show a hierarchical
organization in information processing (Tardif and Clarke,
2011), from highly specialized core regions to more integrated
tertiary para-belt regions. This is confirmed by functional
MRI studies, which suggest a gradient of increasingly more
complex and abstracted processing from primary to higher-order
auditory regions (Rauschecker et al., 1995; Humphries et al.,
2014). Direct connections from MGN to secondary regions have
been shown in monkeys (Rauschecker et al., 1997), suggesting
that this functional organization might be maintained in the
topographical organization of the AR fibers. At its present
stage, tractography can locate and delineate the profile of
major WM bundles with some accuracy, but it is very difficult
to achieve precise site-to-site connectivity analysis with it;
this limits the *in vivo* investigation of the WM topographical
organization of the human brain. However, some studies use
diffusion tractography to parcellate functionally different cortical
regions (Rushworth et al., 2006; Anwander et al., 2007) and
investigate the topographical organization of major bundles (Lee
et al., 2016), and new methods have been proposed to advance
the use of tractography for this purpose (Aydogan and Shi,
2016). In this scenario, it would be interesting to investigate
whether some language-specific connections exist inside the
AR and whether these project to higher-order language-
specific cortical regions. Moreover, this would also allow for
the investigation of whether the tonotopical organization
of the primary auditory cortex is reflected in its thalamo-
cortical connections, as was recently shown in the mouse
brain (Hackett et al., 2011). As dMRI acquisition (in particular,
spatial resolution), diffusion modeling and tractography
techniques improve, we will be able to bridge the gap between
the micro-anatomical knowledge we have of the thalamo-
cortical connections in animals and the macro-anatomical
description in humans.

Language and Hearing Disorders

Damage to the auditory regions, most often the result
of brain infarct or traumatic injury, has been associated
generally with rare auditory syndromes, such as verbal auditory
agnosia (Shivashankar et al., 2001), environmental auditory
agnosia (Taniwaki et al., 2000), and cerebral (or central)
deafness (Griffiths, 2002). However, until now, only one study
investigated the extent of WM damage to the AR in a
patient suffering from verbal auditory agnosia (Maffei et al.,
2017). Investigating the extent of damage to the AR in
patients suffering speech-related comprehension deficits would
potentially enhance our understanding of the involvement of the
AR in language processing.

Also, there is evidence that AR infarct can cause auditory
hallucination (Woo et al., 2014), and that the extra-lemniscal
pathway might be implicated in tinnitus perception (Moller
et al., 1992). At present, studies investigating the auditory

913 pathways in these patients relied on WM ROI measurements
 914 (Lee et al., 2007; Lin et al., 2008), which only outline
 915 a portion of the underlying WM bundles and may not
 916 be representative of the entire tract. Being able to better
 917 understand the dynamics and location of such changes in
 918 the auditory pathways could help inform pathophysiological
 919 treatment strategies, such as repetitive transcranial stimulation
 920 (Langguth et al., 2010).

921 In congenitally and early deaf subjects, volumetric studies have
 922 outlined differences in gray and white matter of the auditory
 923 regions, compared to hearing subjects (Shibata, 2007; Kim et al.,
 924 2009), but to the best of our knowledge, no specific study on
 925 the AR in deaf subjects has been conducted to date. In addition
 926 to providing more detailed information on the anatomical
 927 changes occurring in the brain as a consequence of sensory
 928 deprivation, tractography of the AR may serve as an additional
 929 early diagnostic as well as complementary treatment tool in
 930 monitoring data in congenital hearing loss. This would help
 931 avoid delayed diagnosis that might lead to poor speech outcomes
 932 (Dedhia et al., 2018). Moreover, AR tractography reconstruction
 933 might be fundamental in assessing auditory pathway integrity
 934 before and after cochlear implantation, potentially predicting
 935 implant success (Huang et al., 2015).

936 The structural-functional relationship in language and hearing
 937 disorders can be further investigated by combining tractography
 938 reconstructions and more recently developed diffusion measures
 939 (Raffelt et al., 2012; Calamuneri et al., 2018) within both
 940 classical and more advanced tractography frameworks (Daducci
 941 et al., 2016). The application of these methods in clinical
 942 populations in the context of hearing disorders may help
 943 characterize axonal and myelination diseases (Ohno and Ikenaka,
 944 2018) and auditory neuropathies (Moser and Starr, 2016;
 945 Ohno and Ikenaka, 2018).

946 Tractography reconstruction of the AR could help us
 947 investigate the anatomy of this tract in patients with hearing
 948 and/or language disorders, understand whether these fibers
 949 undergo structural reorganization in the case of auditory
 950 deprivation, and clarify the extent of AR damage in post-
 951 stroke lesion profiles. This may be critical for shedding light
 952 on the functional-structural relationships of linguistic and non-
 953 linguistic sound processing in the human brain.

954 Brain Surgical Planning

955 Investigating the functional and anatomical characteristics of
 956 the auditory fibers reaching the cortex, especially in relation to
 957 their implications for language function, would be important for
 958 surgical planning, such as in the case of tumor or epilepsy surgery
 959 (Wu et al., 2007; Farshidfar et al., 2014). The 3D reconstruction
 960 of major WM bundles is employed to plan and guide resections
 961 during surgery, and a functional atlas of human WM to drive
 962 well balanced onco-functional resections has been proposed
 963 recently (Sarubbo et al., 2015). In this context, diffusion-based
 964 virtual dissections have focused almost exclusively on language
 965 and sensory-motor structures (Chen et al., 2015). Possible
 966 reasons why AR fibers have not received much attention in
 967 the neurosurgical literature include the possibility that most
 968 of the non-linguistic auditory processing may happen at the

970 brain-stem level and that auditory information is conveyed to
 971 both hemispheres, so that extensive bilateral damage is necessary
 972 for complete deafness (Griffiths, 2002). However, different
 973 sub-modal aspects of auditory processing, for example, those
 974 related to music perception and/or speech comprehension,
 975 might depend on the integrity of these projections (Hayashi
 976 and Hayashi, 2007; Baird et al., 2014). For cases of temporal
 977 lobe resection, the reliable virtual reconstruction of the AR
 978 might be critical for minimizing post-operative deficits in these
 979 domains. Also, it might serve in pre-operative assessments for
 980 cochlear implantation, as hearing recovery after implantation
 981 is influenced by the integrity of subcortical pathways
 982 (Vlastarakos et al., 2010).

983 Brain Radiation Oncology Planning

984 Today, X-ray therapy (XRT) is the standard of care for most
 985 brain tumors. However, XRT can damage normal brain tissue,
 986 causing neurocognitive deficits in different cognitive domains
 987 (Makale et al., 2016). The consideration of neuroimaging
 988 techniques for treatment planning is gaining importance as it
 989 helps avoid such complications by minimizing the unnecessary
 990 absorption of radiation in sensitive regions outside the tumor.
 991 Nevertheless, further improvement of radiation treatment will
 992 require tailored radiotherapy based on intra-treatment response
 993 (Wong et al., 2017).

994 Additionally, studies have shown XRT side effects in both
 995 gray (Bahrami et al., 2017) and white matter, although it is
 996 still largely unclear how variable sensitivity to radiation injury
 997 is across various regions of the brain (Connor et al., 2017).
 998 Kawasaki et al. (2017) show that tractography can help evaluate
 999 how radiation from XRT differentially affects WM regions and
 1000 pathways. This knowledge, together with an understanding of
 1001 how damage to such regions and pathways affects cognitive
 1002 processes, could be used in the future to further optimize
 1003 radiation treatment planning.

1004 CONCLUSION

1005 The anatomical and functional organization of the auditory
 1006 system is still not well understood, particularly in humans.
 1007 Successful *in vivo* tractographic reconstruction of the human
 1008 auditory tracts is of great importance for clinical applications
 1009 (e.g., pre-surgical mapping), as well as for basic research (e.g.,
 1010 language and auditory systems). This review outlines how the
 1011 characterization of the AR has been limited by the methods
 1012 used in the past and how advances in MRI acquisition and
 1013 diffusion tractography methods offer the possibility to improve
 1014 the characterization of this important WM tract. A few exciting
 1015 potential research areas are suggested that would investigate
 1016 anatomy and function concurrently in the same individual, both
 1017 in health (e.g., the role of these tracts in language processing)
 1018 and in disease (e.g., how the integrity of this tract relates to cognitive
 1019 deficits). However, in order to obtain reliable reconstructions
 1020 of the AR across subjects and protocols, additional work is
 1021 needed to better understand how diffusion MRI acquisition
 1022

1027 and tractography reconstruction strategies affect the AR 3D
1028 characterization and to validate tractography reconstructions at
1029 a micro-anatomical scale. Furthermore, as diffusion tractography
1030 is blind to the directionality of reconstructed fibers, the
1031 AR bundle could include both thalamo-cortical and cortico-
1032 thalamic projections, and therefore more studies are needed to
1033 differentiate between the afferent or efferent nature of these
1034 connections. Although these methodological challenges apply to
1035 diffusion MRI tractography in general, here we have focused on
1036 their relevance to the AR, a tract that has proven to be rather
1037 elusive for the reasons herein reviewed.

1040 REFERENCES

1041 Aganj, I., Lenglet, C., Sapiro, G., Yacoub, E., Ugurbil, K., and Harel, N. (2010).
1042 Reconstruction of the orientation distribution function in single- and multiple-
1043 shell q-ball imaging within constant solid angle. *Magn. Reson. Med.* 64, 554–566.
1044 doi: 10.1002/mrm.22365

1045 Anwender, A., Tittgemeyer, M., von Cramon, D. Y., Friederici, A. D., and Knösche,
1046 T. R. (2007). Connectivity-based parcellation of broca's area. *Cereb. Cortex* 17,
1047 816–825. doi: 10.1093/cercor/bhk034

1048 Aydogan, D. B., and Shi, Y. (2016). Probabilistic tractography for topographically
1049 organized connectomes. *Med. Image Comput. Assist. Interv.* 9900,
1050 201–209. doi: 10.1007/978-3-319-46720-7_24

1051 Bahrami, N., Seibert, T. M., Karunamuni, R., Bartsch, H., Krishnan, A., Farid, N.,
1052 et al. (2017). Altered network topology in patients with primary brain tumors
1053 after fractionated radiotherapy. *Brain Connect.* 7, 299–308. doi: 10.1089/brain.
1054 2017.0494

1055 Baird, A. D., Walker, D. G., Biggs, V., and Robinson, G. A. (2014). Selective
1056 preservation of the beat in apperceptive music agnosia: a case study. *Cortex* 53,
1057 27–33. doi: 10.1016/J.CORTEX.2014.01.005

1058 Basser, P., Mattiello, J., and LeBihan, D. (1994). MR diffusion tensor spectroscopy
1059 and imaging. *Biophys. J.* 66, 259–267. doi: 10.1016/S0006-3495(94)80775-1

1060 Baumann, S., Petkov, C. I., and Griffiths, T. D. (2013). A unified framework for
1061 the organization of the primate auditory cortex. *Front. Syst. Neurosci.* 7:11.
1062 doi: 10.3389/fnsys.2013.00011

1063 Behrens, T., Woolrich, M., Jenkinson, M., Johansen-Berg, H., Nunes, R., Clare, S.,
1064 et al. (2003). Characterization and propagation of uncertainty in diffusion-
1065 weighted MR imaging. *Magn. Reson. Med.* 50, 1077–1088. doi: 10.1002/mrm.
1066 10609

1067 Behrens, T. E. J., Berg, H. J., Jbabdi, S., Rushworth, M. F. S., and Woolrich, M. W.
1068 (2007). Probabilistic diffusion tractography with multiple fibre orientations:
1069 what can we gain? *Neuroimage* 34, 144–155. doi: 10.1016/j.neuroimage.2006.
1070 09.018

1071 Berman, J. I., Lanza, M. R., Blaskey, L., Edgar, J. C., and Roberts, T. P. L. (2013).
1072 High angular resolution diffusion imaging probabilistic tractography of the
1073 auditory radiation. *Am. J. Neuroradiol.* 34, 1573–1578. doi: 10.3174/ajnr.A3471

1074 Brugge, J. (2013). Anatomy and physiology of auditory pathways and cortex.
1075 *Handb. Clin. Neurophysiol.* 10, 25–52. doi: 10.1016/B978-0-7020-5310-8.
1076 00002-8

1077 Bürgel, U., Amunts, K., Hoemke, L., Mohlberg, H., Gilsbach, J. M., and Zilles, K.
1078 (2006). White matter fiber tracts of the human brain: three-dimensional
1079 mapping at microscopic resolution, topography and intersubject variability.
1080 *Neuroimage* 29, 1092–1105. doi: 10.1016/j.neuroimage.2005.08.040

1081 Burton, H., and Jones, E. G. (1976). The posterior thalamic region and its cortical
1082 projection in new world and old world monkeys. *J. Comp. Neurol.* 168, 249–301.
1083 doi: 10.1002/cne.901680204

1084 Calamuneri, A., Arrigo, A., Mormina, E., Milardi, D., Cacciola, A., Chillemi, G.,
1085 et al. (2018). White matter tissue quantification at low b-values within
1086 constrained spherical deconvolution framework. *Front. Neurol.* 9:716. doi: 10.
1087 3389/fneur.2018.00716

1088 Catani, M., Allin, M. P. G., Husain, M., Pugliese, L., Mesulam, M. M., Murray,
1089 R. M., et al. (2007). Symmetries in human brain language pathways correlate
1090 with verbal recall. *Proc. Natl. Acad. Sci. U.S.A.* 104, 17163–17168. doi: 10.1073/
1091 pnas.0702116104

AUTHOR CONTRIBUTIONS

JJ conceived of the review. SS revised the manuscript for neuro-
anatomical content. CM drafted the manuscript and designed the
figures. All authors contributed to the final manuscript.

ACKNOWLEDGMENTS

We thank Albert Galaburda for his insightful comments on a
previous version of this manuscript.

Catani, M., and de Schotten, M. (2008). A diffusion tensor imaging tractography
atlas for virtual in vivo dissections. *Cortex* 44, 1105–1132. doi: 10.1016/j.cortex.
2008.05.004

Catani, M., Howard, R. J., Pajevic, S., and Jones, D. K. (2002). Virtual in vivo
interactive dissection of white matter fasciculi in the human brain. *neuroimage*
17, 77–94. doi: 10.1006/nimg.2002.1136

Catani, M., and Thiebaut de Schotten, M. (2008). A diffusion tensor imaging
tractography atlas for virtual in vivo dissections. *Cortex* 44, 1105–1132. doi:
10.1016/j.cortex.2008.05.004

Chang, Y., Lee, S., Hwang, M., Bae, S., Kim, M., Lee, J., et al. (2004). Auditory
neural pathway evaluation on sensorineural hearing loss using diffusion
tensor imaging. *Neuroreport* 15, 1699–1703. doi: 10.1097/01.wnr.0000134584.
10207

Chen, Z., Tie, Y., Olubiyi, O., Rigolo, L., Mehrtash, A., Norton, I., et al. (2015).
Reconstruction of the arcuate fasciculus for surgical planning in the setting
of peritumoral edema using two-tensor unscented Kalman filter tractography.
Neuroimage 7, 815–822. doi: 10.1016/j.nicl.2015.03.009

Connor, M., Karunamuni, R., McDonald, C., Seibert, T., White, N., Moiseenko, V.,
et al. (2017). Regional susceptibility to dose-dependent white matter damage
after brain radiotherapy. *Radiother. Oncol.* 123, 209–217. doi: 10.1016/j.radonc.
2017.04.006

Crippa, A., Lanting, C. P., van Dijk, P., and Roerdink, J. B. T. M. (2010). A diffusion
tensor imaging study on the auditory system and tinnitus. *Open Neuroimaging*
J. 4, 16–25. doi: 10.2174/1874440001004010016

Daducci, A., Dal Palú, A., Descoteaux, M., and Thiran, J.-P. (2016). Microstructure
informed tractography: pitfalls and open challenges. *Front. Neurosci.* 10:247.
doi: 10.3389/fnins.2016.00247

De Benedictis, A., Petit, L., Descoteaux, M., Marras, C. E., Barbareschi, M.,
Corsini, F., et al. (2016). New insights in the homotopic and heterotopic
connectivity of the frontal portion of the human corpus callosum revealed by
microdissection and diffusion tractography. *Hum. Brain Mapp.* 37, 4718–4735.
doi: 10.1002/hbm.23339

de la Mothe, L., Blumell, S., Kajikawa, Y., and Hackett, T. (2006). Thalamic
connections of the auditory cortex in marmoset monkeys: core and medial belt
regions. *J. Comp. Neurol.* 496, 72–96. doi: 10.1002/cne.20924

Dedhia, K., Graham, E., and Park, A. (2018). Hearing loss and failed newborn
hearing screen. *Clin. Perinatol.* 45, 629–643. doi: 10.1016/j.clp.2018.07.004

Dejerine, J., and Dejerine-Klumpke, A. (1895). *Anatomie Des Centres Nerveux*.
Paris: Rueff et Cie.

Dell'Acqua, F., and Catani, M. (2012). Structural human brain networks: hot topics
in diffusion tractography. *Curr. Opin. Neurol.* 25, 375–383. doi: 10.1097/WCO.
0b013e328355d544

Descoteaux, M., Deriche, R., Knösche, T., and Anwender, A. (2009). Deterministic
and probabilistic tractography based on complex fiber orientation distributions.
IEEE Trans. Med. Imaging 28, 269–286. doi: 10.1109/TMI.2008.2004424

Fan, Q., Witzel, T., Nummenmaa, A., Van Dijk, K. R. A., Van Horn, J. D., Drews,
M. K., et al. (2015). MGH-USC human connectome project datasets with
ultra-high b-value diffusion MRI. *Neuroimage* 124, 1108–1114. doi: 10.1016/j.
neuroimage.2015.08.075

Farshidfar, Z., Faeghi, F., Mohseni, M., Seddighi, A., Kharrazi, H. H., and
Abdolmohammadi, J. (2014). Diffusion tensor tractography in the presurgical
assessment of cerebral gliomas. *Neuroradiol. J.* 27, 75–84. doi: 10.15274/NRJ-
2014-10008

- 1141 Fernaindez-Miranda, J. C., Wang, Y., Pathak, S., Stefaneau, L., Verstynen, T.,
1142 and Yeh, F. F. C. (2015). Asymmetry, connectivity, and segmentation of the
1143 arcuate fascicle in the human brain. *Brain Struct. Funct.* 220, 1665–1680. doi:
10.1007/s00429-014-0751-7
- 1144 Flechsig, P. (1920). *Anatomie Des Menschlichen Gehirns Und Rücken-marks Auf*
1145 *Myelogenetischer Grundlage*. Leipzig: Georg Thieme Verlag.
- 1146 Friederici, A. D. (2009). Pathways to language: fiber tracts in the human brain.
1147 *Trends Cogn. Sci.* 13, 175–181. doi: 10.1016/j.tics.2009.01.001
- 1148 Fullerton, B. C., and Pandya, D. N. (2007). Architectonic analysis of the auditory-
1149 related areas of the superior temporal region in human brain. *J. Comp. Neurol.*
504, 470–498. doi: 10.1002/cne.21432
- 1150 Galaburda, A. M., LeMay, M., Kemper, T. L., and Geschwind, N. (1978). Right-left
1151 asymmetries in the brain. *Science* 199, 852–856. doi: 10.1126/science.341314
- 1152 Galaburda, A. M., and Pandya, D. N. (1983). The intrinsic architectonic and
1153 connective organization of the superior temporal region of the rhesus
1154 monkey. *J. Comp. Neurol.* 221, 169–184. doi: 10.1002/cne.902210206
- 1155 Galaburda, A. M., and Sanides, F. (1980). Cytoarchitectonic organization of the
1156 human auditory cortex. *J. Comp. Neurol.* 190, 597–610. doi: 10.1002/cne.
901900312
- 1157 Geschwind, N., and Galaburda, A. M. (1985). Cerebral lateralization. Biological
1158 mechanisms, associations, and pathology: I. A hypothesis and a program
1159 for research. *Arch. Neurol.* 42, 428–459. doi: 10.1001/archneur.1985.0406
0050026008
- 1160 Griffiths, T. D. (2002). Central auditory pathologies. *Br. Med. Bull.* 63, 107–120.
1161 doi: 10.1093/bmb/63.1.107
- 1162 Hackett, T. A., Barkat, T. R., O'Brien, B. M. J., Hensch, T. K., and Polley, D. B.
1163 (2011). Linking topography to tonotopy in the mouse auditory thalamocortical
1164 circuit. *J. Neurosci.* 31, 2983–2995. doi: 10.1523/JNEUROSCI.5333-10.2011
- 1165 Hackett, T. A., Preuss, T. M., and Kaas, J. H. (2001). Architectonic identification
1166 of the core region in auditory cortex of macaques, chimpanzees, and humans.
1167 *J. Comp. Neurol.* 441, 197–222. doi: 10.1002/cne.1407
- 1168 Hackett, T. A., Stepniewska, I., and Kaas, J. H. (1998). Thalamocortical connections
1169 of the parabelt auditory cortex in macaque monkeys. *J. Comp. Neurol.* 400,
271–286. doi: 10.1002/(SICI)1096-9861(19981019)400:2<271::AID-CNE8>3.0.
CO;2-6
- 1170 Hashikawa, T., Molinari, M., Rausell, E., and Jones, E. (1995). Patchy and laminar
1171 terminations of medial geniculate axons in monkey auditory cortex. *J. Comp.*
1172 *Neurol.* 362, 195–208. doi: 10.1002/cne.903620204
- 1173 Hayashi, K., and Hayashi, R. (2007). Pure word deafness due to left subcortical
1174 lesion: neurophysiological studies of two patients. *Clin. Neurophysiol.* 118,
863–868. doi: 10.1016/j.clinph.2007.01.002
- 1175 Hickok, G., and Poeppel, D. (2007). The cortical organization of speech processing.
1176 *Nat. Rev. Neurosci.* 8, 393–402. doi: 10.1038/nrn2113
- 1177 Hornickel, J., Skoe, E., and Kraus, N. (2009). Subcortical laterality of speech
1178 encoding. *Audiol. Neuro Otol.* 14, 198–207. doi: 10.1159/000188533
- 1179 Huang, L., Zheng, W., Wu, C., Wei, X., Wu, X., Wang, Y., et al. (2015). Diffusion
1180 tensor imaging of the auditory neural pathway for clinical outcome of cochlear
1181 implantation in pediatric congenital sensorineural hearing loss patients. *PLoS*
1182 *One* 10:e0140643. doi: 10.1371/journal.pone.0140643
- 1183 Humphries, C., Sabri, M., Lewis, K., and Liebenthal, E. (2014). Hierarchical
1184 organization of speech perception in human auditory cortex. *Front. Neurosci.*
8:406. doi: 10.3389/fnins.2014.00406
- 1185 Iglesias, J. E., Insausti, R., Lerma-Usabiaga, G., Bocchetta, M., Van Leemput, K.,
1186 and Paz-Alonso, P. M. (2018). A probabilistic atlas of the human thalamic
1187 nuclei combining ex vivo MRI, and histology. *Neuroimage* 183, 314–326. doi:
10.1016/j.neuroimage.2018.08.012
- 1188 Javad, F., Warren, J., Micallef, C., Thornton, J., Golay, X., Yousry, T., et al. (2014).
1189 Auditory tracts identified with combined fMRI and diffusion tractography.
1190 *Neuroimage* 84, 562–574. doi: 10.1016/j.neuroimage.2013.09.007
- 1191 Jeurissen, B., Leemans, A., Tournier, J. D., Jones, D. K., and Sijbers, J. (2013).
1192 Investigating the prevalence of complex fiber configurations in white matter
1193 tissue with diffusion magnetic resonance imaging. *Hum. Brain Mapp.* 34,
2747–2766. doi: 10.1002/hbm.22099
- 1194 Jones, D. K., and Cercignani, M. (2010). Twenty-five pitfalls in the analysis of
1195 diffusion MRI data. *NMR Biomed.* 23, 803–820. doi: 10.1002/nbm.1543
- 1196 Jones, E. G. (2003). Chemically defined parallel pathways in the monkey auditory
1197 system. *Ann. N. Y. Acad. Sci.* 999, 218–233. doi: 10.1196/annals.1284.033
- Kaas, J. H., and Hackett, T. A. (2000). Subdivisions of auditory cortex and
processing streams in primates. *Proc. Natl. Acad. Sci. U.S.A.* 97, 11793–11799.
doi: 10.1073/pnas.97.22.11793
- Kim, D.-J., Park, S.-Y., Kim, J., Lee, D. H., and Park, H.-J. (2009). Alterations of
white matter diffusion anisotropy in early deafness. *Neuroreport* 20, 1032–1036.
doi: 10.1097/WNR.0b013e32832e0cdd
- Kitajima, M., Hirai, T., Yoneda, T., Iryo, Y., Azuma, M., Tateishi, M., et al. (2015).
Visualization of the medial and lateral geniculate nucleus on phase difference
enhanced imaging. *Am. J. Neuroradiol.* 36, 1669–1674. doi: 10.3174/ajnr.
A4356
- Langguth, B., Kleinjung, T., Landgrebe, M., de Ridder, D., and Hajak, G. (2010).
rTMS for the treatment of tinnitus: the role of neuronavigation for coil
positioning. *Neurophysiol. Clin.* 40, 45–58. doi: 10.1016/j.neucli.2009.03.001
- Lawes, I. N. C., Barrick, T. R., Murugam, V., Spierings, N., Evans, D. R.,
Song, M., et al. (2008). Atlas-based segmentation of white matter tracts of the
human brain using diffusion tensor tractography and comparison with classical
dissection. *Neuroimage* 39, 62–79. doi: 10.1016/j.neuroimage.2007.06.041
- Lee, C., and Winer, J. (2008). Connections of cat auditory cortex: III.
Corticocortical system. *J. Comp. Neurol.* 507, 1920–1943. doi: 10.1002/cne.
21613
- Lee, C. C., and Sherman, S. M. (2010). Topography and physiology of ascending
streams in the auditory tectothalamic pathway. *Proc. Natl. Acad. Sci. U.S.A.* 107,
372–377. doi: 10.1073/pnas.0907873107
- Lee, D. H., Lee, D. W., and Han, B. S. (2016). Topographic organization of motor
fiber tracts in the human brain: findings in multiple locations using magnetic
resonance diffusion tensor tractography. *Eur. Radiol.* 26, 1751–1759. doi: 10.
1007/s00330-015-3989-4
- Lee, Y. J., Bae, S. J., Lee, S. H., Lee, J. J., Lee, K. Y., Kim, M. N., et al. (2007).
Evaluation of white matter structures in patients with tinnitus using diffusion
tensor imaging. *J. Clin. Neurosci.* 14, 515–519. doi: 10.1016/j.jocn.2006.10.002
- Lin, Y., Wang, J., Wu, C., Wai, Y., Yu, J., and Ng, S. (2008). Diffusion tensor
imaging of the auditory pathway in sensorineural hearing loss: changes in
radial diffusivity and diffusion anisotropy. *J. Magn. Reson. Imaging* 28, 598–603.
doi: 10.1002/jmri.21464
- Ludwig, E., and Klingler, J. (1956). *Atlas Cerebri Humani. The Inner Structure of the*
Brain Demonstrated on the Basis of Macroscopical Preparations. Boston, MA:
Little, Brown and Company.
- Luehke, L. E., Krubitzer, L. A., and Kaas, J. H. (1989). Connections of primary
auditory cortex in the new world monkey, *Saguinus*. *J. Comp. Neurol.* 285,
487–513. doi: 10.1002/cne.902850406
- Maffei, C., Capasso, R., Cazzoli, G., Colosimo, C., Dell'Acqua, F., Piludu, F., et al.
(2017). Pure word deafness following left temporal damage: behavioral and
neuroanatomical evidence from a new case. *Cortex* 97, 240–254. doi: 10.1016/j.
cortex.2017.10.006
- Maffei, C., Jovicich, J., de Benedictis, A., Corsini, F., Barbareschi, M., Chioffi, F.,
et al. (2018). Topography of the human acoustic radiation as revealed by ex vivo
fibers micro-dissection and in vivo diffusion-based tractography. *Brain Struct.*
Funct. 223, 449–459. doi: 10.1007/s00429-017-1471-6
- Maier-Hein, K. H., Neher, P. F., Houde, J.-C., Côté, M.-A., Garyfallidis, E.,
Zhong, J., et al. (2017). The challenge of mapping the human connectome
based on diffusion tractography. *Nat. Commun.* 8:1349. doi: 10.1038/s41467-
017-01285-x
- Makale, M. T., McDonald, C. R., Hattangadi-Gluth, J. A., and Kesari, S. (2016).
Mechanisms of radiotherapy-associated cognitive disability in patients with
brain tumours. *Nat. Rev. Neurol.* 13, 52–64. doi: 10.1038/nrneurol.2016.185
- Merzenich, M. M., and Brugge, J. F. (1973). Representation of the cochlear partition
of the superior temporal plane of the macaque monkey. *Brain Res.* 50, 275–296.
doi: 10.1016/0006-8993(73)90731-2
- Mesulam, M. M. (1979). Tracing neuronal connections of human brain with
selective silver impregnation. Observations on geniculocalcarine, spinothalamic
and entorhinal pathways. *Arch. Neurol.* 36, 814–818. doi: 10.1001/archneur.
1979.00500490028004
- Mesulam, M. M., and Pandya, D. N. (1973). The projections of the medial
geniculate complex within the sylvian fissure of the rhesus monkey. *Brain Res.*
60, 315–333. doi: 10.1016/0006-8993(73)90793-2
- Minkowski, M. (1923). Etude sur les connexions anatomiques des circonvolutions
rolandiques. *Arch. Neurol. Psychiatr.* 12, 227–268.

- 1255 Molinari, M., Dell'Anna, M., Rausell, E., Leggio, M., Hashikawa, T., and Jones, E.
1256 (1995). Auditory thalamocortical pathways defined in monkeys by calcium-
1257 binding protein immunoreactivity. *J. Comp. Neurol.* 362, 171–194. doi: 10.1002/
1258 cne.903620203
- 1259 Moller, A. R. (2006). *Hearing: Anatomy, Physiology, and Disorders of the Auditory
1260 System. Second Edition.* Cambridge, MA: Academic Press.
- 1261 Moller, A. R., Moller, M. B., and Yokota, M. (1992). Some forms of tinnitus may
1262 involve the extralemnisal auditory pathway.pdf. *Laryngoscope* 102, 1165–1171.
1263 doi: 10.1288/00005537-199210000-00012
- 1264 Morel, A., Garraghty, P. E., and Kaas, J. H. (1993). Tonotopic organization,
1265 architectonic fields, and connections of auditory cortex in macaque monkeys.
1266 *J. Comp. Neurol.* 335, 437–459. doi: 10.1002/cne.903350312
- 1267 Morel, A., and Kaas, J. (1992). Subdivisions and connections of auditory
1268 cortex in owl monkeys. *J. Comp. Neurol.* 318, 27–63. doi: 10.1002/cne.9031
1269 80104
- 1270 Mori, S., Crain, B. J., Chacko, V. P., and van Zijl, P. C. (1999). Three-dimensional
1271 tracking of axonal projections in the brain by magnetic resonance imaging. *Ann.
1272 Neurol.* 45, 265–269. doi: 10.1002/1531-8249(199902)45:2
- 1273 Moser, T., and Starr, A. (2016). Auditory neuropathy neural and synaptic
1274 mechanisms. *Nat. Rev. Neurol.* 12, 135–149. doi: 10.1038/nrneuro.2016.10
- 1275 Ohno, N., and Ikenaka, K. (2018). Axonal and neuronal degeneration in myelin
1276 diseases. *Neurosci. Res.* 139, 48–57. doi: 10.1016/j.neures.2018.08.013
- 1277 Pascalau, R., Popa, S. R., Sfrângeu, S., and Szabo, B. (2018). Anatomy of the limbic
1278 white matter tracts as revealed by fiber dissection and tractography. *World
1279 Neurosurg.* 113, 672–689. doi: 10.1016/j.wneu.2018.02.121
- 1280 Passingham, R. (2009). How good is the macaque monkey model of the
1281 human brain? *Curr. Opin. Neurobiol.* 19, 6–11. doi: 10.1016/j.conb.2009.
1282 01.002
- 1283 Penhune, V. B., Zatorre, R. J., and Macdonald, J. D. (1996). Interhemispheric
1284 anatomical differences in human primary auditory cortex?: probabilistic
1285 mapping and volume measurement from magnetic resonance scans. *Cereb.
1286 Cortex* 6, 661–672. doi: 10.1093/cercor/6.5.661
- 1287 Pfeifer, R. (1920). *Myelogenetisch-anatomische Untersuchungen Über Das Kortikale
1288 Ende Der Horleitung.* Leipzig: BG Teubner.
- 1289 Poeppel, D. (2003). The analysis of speech in different temporal integration
1290 windows: cerebral lateralization as “asymmetric sampling in time.”. *Speech
1291 Commun.* 41, 245–255. doi: 10.1016/S0167-6393(02)00107-3
- 1292 Polyak, S. (1932). *The Main Afferent Fiber Systems of the Cerebral Cortex in
1293 Primates, Vol. Vol 2.* Berkeley, CA: University of California Press, 396.
- 1294 Profant, O., Škoch, A., Balogová, Z., Tintira, J., Hlinka, J., and Syka, J. (2014).
1295 Diffusion tensor imaging and MR morphometry of the central auditory
1296 pathway and auditory cortex in aging. *Neuroscience* 260, 87–97. doi: 10.1016/
1297 j.neuroscience.2013.12.010
- 1298 Rademacher, J., Bürgel, U., and Zilles, K. (2002). Stereotaxic localization,
1299 intersubject variability, and interhemispheric differences of the human auditory
1300 thalamocortical system. *Neuroimage* 17, 142–160. doi: 10.1006/nimg.2002.
1301 1178
- 1302 Rademacher, J., Morosan, P., Schormann, T., Schleicher, A., Werner, C., Freund,
1303 H.-J., et al. (2001). Probabilistic mapping and volume measurement of human
1304 primary auditory cortex. *Neuroimage* 13, 669–683. doi: 10.1006/nimg.2000.
1305 0714
- 1306 Raffelt, D., Tournier, J. D., Rose, S., Ridgway, G. R., Henderson, R., Crozier, S., et al.
1307 (2012). Apparent fibre density: a novel measure for the analysis of diffusion-
1308 weighted magnetic resonance images. *Neuroimage* 59, 3976–3994. doi: 10.1016/
1309 j.neuroimage.2011.10.045
- 1310 Rauschecker, J. P., Tian, B., and Hauser, M. (1995). Processing of complex sounds
1311 in the macaque nonprimary auditory cortex. *Science* 268, 111–114. doi: 10.1126/
1312 science.7701330
- 1313 Rauschecker, J. P., Tian, B., Pons, T., and Mishkin, M. (1997). Serial and parallel
1314 processing in rhesus monkey auditory cortex. *J. Comp. Neurol.* 382, 89–103.
1315 doi: 10.1002/(SICI)1096-9861(19970526)382:1<89::AID-CNE6>3.0.CO;2-G
- 1316 Renaud, E., Descoteaux, M., Bernier, M., Garyfallidis, E., and Whittingstall, K.
1317 (2016). Semi-automatic segmentation of optic radiations and LGN, and their
1318 relationship to EEG alpha waves. *PLoS One* 11:e156436. doi: 10.1371/journal.
1319 pone.0156436
- 1320 Rheault, F., St-Onge, E., Sidhu, J., Maier-Hein, K., Tzourio-Mazoyer, N., Petit, L.,
1321 et al. (2019). Bundle-specific tractography with incorporated anatomical and
1322 orientational priors. *Neuroimage* 186, 382–398. doi: 10.1016/j.neuroimage.
1323 2018.11.018
- 1324 Rushworth, M. F. S., Behrens, T. E. J., and Johansen-Berg, H. (2006). Connection
1325 patterns distinguish 3 regions of human parietal cortex. *Cereb. Cortex* 16,
1326 1418–1430. doi: 10.1093/cercor/bhj079
- 1327 Sarubbo, S., De Benedictis, A., Merler, S., Mandonnet, E., Balbi, S., Granieri, E.,
1328 et al. (2015). Towards a functional atlas of human white matter. *Hum. Brain
1329 Mapp.* 36, 3117–3136. doi: 10.1002/hbm.22832
- 1330 Saur, D., Kreher, B. W., Schnell, S., Kümmerer, D., Kellmeyer, P., Vry, M.-S., et al.
1331 (2008). Ventral and dorsal pathways for language. *Proc. Natl. Acad. Sci. U.S.A.*
1332 105, 18035–18040. doi: 10.1073/pnas.0805234105
- 1333 Schmahmann, J. D., Pandya, D. N., Wang, R., Dai, G., D'Arceuil, H. E., De
1334 Crespigny, A. J., et al. (2007). Association fibre pathways of the brain: parallel
1335 observations from diffusion spectrum imaging and autoradiography. *Brain* 130,
1336 630–653. doi: 10.1093/brain/awl359
- 1337 Seldon, H. L. (1981). Structure of human auditory cortex. I. Cytoarchitectonics and
1338 dendritic distributions. *Brain Res.* 229, 277–294. doi: 10.1016/0006-8993(81)
1339 90994-X
- 1340 Shibata, D. K. (2007). Differences in brain structure in deaf persons on MR imaging
1341 studied with voxel-based morphometry. *Am. J. Neuroradiol.* 28, 243–249.
- 1342 Shivashankar, N., Shashikala, H. R., Nagaraja, D., Jayakumar, P. N., and
1343 Ratnavalli, E. (2001). Pure word deafness in two patients with subcortical
1344 lesions. *Clin. Neurol. Neurosurg.* 103, 201–205. doi: 10.1016/S0303-8467(01)
1345 00136-6
- 1346 Taniwaki, T., Tagawa, K., Sato, F., and Iino, K. (2000). Auditory agnosia restricted
1347 to environmental sounds following cortical deafness and generalized auditory
1348 agnosia. *Clin. Neurol. Neurosurg.* 102, 156–162. doi: 10.1016/S0303-8467(00)
1349 00090-1
- 1350 Tardif, E., and Clarke, S. (2001). Intrinsic connectivity of human auditory areas:
1351 a tracing study with DiI. *Eur. J. Neurosci.* 13, 1045–1050. doi: 10.1046/j.0953-
1352 816x.2001.01456.x
- 1353 Thiebaut de Schotten, M., Dell'Acqua, F., Valabregue, R., and Catani, M. (2012).
1354 Monkey to human comparative anatomy of the frontal lobe association tracts.
1355 *Cortex* 48, 82–96. doi: 10.1016/j.cortex.2011.10.001
- 1356 Thiebaut de Schotten, M., Ffytche, D. H., Bizzi, A., Dell'Acqua, F., Allin, M.,
1357 Walshe, M., et al. (2011). Atlasing location, asymmetry and inter-subject
1358 variability of white matter tracts in the human brain with MR diffusion
1359 tractography. *Neuroimage* 54, 49–59. doi: 10.1016/j.neuroimage.2010.07.055
- 1360 Thomas, C., Ye, F. Q., Irfanoglu, M. O., Modi, P., Saleem, K. S., Leopold, D. A.,
1361 et al. (2014). Anatomical accuracy of brain connections derived from diffusion
1362 MRI tractography is inherently limited. *Proc. Natl. Acad. Sci. U.S.A.* 111,
1363 16574–16579. doi: 10.1073/pnas.1405672111
- 1364 Tournier, J. D., Calamante, F., and Connelly, A. (2013). Determination of the
1365 appropriate b-value and number of gradient directions for high-angular-
1366 resolution diffusion-weighted imaging. *NMR Biomed.* 26, 1775–1786. doi: 10.
1367 1002/nbm.3017
- 1368 Tournier, J.-D., Yeh, C.-H., Calamante, F., Cho, K.-H., Connelly, A., and Lin, C.-
1369 P. (2008). Resolving crossing fibres using constrained spherical deconvolution:
1370 validation using diffusion-weighted imaging phantom data. *Neuroimage* 42,
1371 617–625. doi: 10.1016/j.neuroimage.2008.05.002
- 1372 Tuch, D. S. (2004). Q-ball imaging. *Magn. Reson. Med.* 52, 1358–1372. doi: 10.1002/
1373 mrm.20279
- 1374 Tuch, D. S., Reese, T. G., Wiegell, M. R., Makris, N., Belliveau, J. W., and Wedeen,
1375 V. J. (2002). High angular resolution diffusion imaging reveals intravoxel white
1376 matter heterogeneity. *Magn. Reson. Med.* 48, 577–582. doi: 10.1002/mrm.
1377 10268
- 1378 Vlastarakos, P. V., Nikolopoulos, T. P., Pappas, S., Buchanan, M. A., Bewick, J.,
1379 and Kandiloros, D. (2010). Cochlear implantation update: contemporary
1380 preoperative imaging and future prospects – the dual modality approach as a
1381 standard of care. *Expert Rev. Med. Devices* 7, 555–567. doi: 10.1586/erd.10.28
- 1382 Von Economo, C., and Horn, L. (1930). Über Windungsrelief, Maße und
1383 Rindenarchitektonik der Supratemporalfläche, ihre individuellen und ihre
1384 Seitenunterschiede. *Zeitschrift Für Die Gesamte Neurologie Und Psychiatrie* 130,
1385 678–757. doi: 10.1007/BF02865945
- 1386 von Monakow, C. (1882). Weitere Mitteilungen über die durch Exstir- pation
1387 circumscripiter Hirnrindenregionen bedingte Entwicklung- shemmungen des
1388 Kaninchengehirns. *Arch. Neurol. Psychiatr.* 12:535.
- 1389 Walker, A. E. (1937). The Projection of the Medial Geniculate Body to the Cerebral
1390 Cortex in the Macaque Monkey. *J. Anat.* 71, 319–331.
- 1391 Winer, J., and Lee, C. (2007). The distributed auditory cortex. *Hear. Res.* 229, 3–13.
1392 doi: 10.1016/j.heares.2007.01.017

- 1369 Winer, J. A., Diehl, J. J., and Larue, D. T. (2001). Projections of auditory cortex
1370 to the medial geniculate body of the cat. *J. Comp. Neurol.* 430, 27–55. doi:
1371 10.1002/1096-9861(20010129)430:1<27::AID-CNE1013>3.0.CO;2-8 1426
- 1372 Wong, K. H., Panek, R., Bhide, S. A., Nutting, C. M., Harrington, K. J., and
1373 Newbold, K. L. (2017). The emerging potential of magnetic resonance imaging
1374 in personalizing radiotherapy for head and neck cancer: an oncologist's
1375 perspective. *Br. J. Radiol.* 90:20160768. doi: 10.1259/bjr.20160768 1427
- 1376 Woo, P. Y., Leung, L. N., Cheng, S. T., and Chan, K.-Y. (2014). Monoaural musical
1377 hallucinations caused by a thalamocortical auditory radiation infarct: a case
1378 report. *J. Med. Case Rep.* 8:400. doi: 10.1186/1752-1947-8-400 1428
- 1379 Wu, C. M., Ng, S. H., Wang, J. J., and Liu, T. C. (2009). Diffusion tensor imaging
1380 of the subcortical auditory tract in subjects with congenital cochlear nerve
1381 deficiency. *Am. J. Neuroradiol.* 30, 1773–1777. doi: 10.3174/ajnr.A1681 1429
- 1382 Wu, J.-S., Zhou, L.-F., Tang, W.-J., Mao, Y., Hu, J., Song, Y.-Y., et al. (2007). Clinical
1383 evaluation and follow-up outcome of diffusion tensor imaging-based functional
1384 neuronavigation. *Neurosurgery* 61, 935–949. doi: 10.1227/01.neu.0000303189.
1385 80049.ab 1430
- 1386 Yeh, F. C., Panesar, S., Fernandes, D., Meola, A., Yoshino, M., Fernandez-Miranda,
1387 J. C., et al. (2018). Population-averaged atlas of the macroscale human structural
1388 connectome and its network topology. *Neuroimage* 178, 57–68. doi: 10.1016/j.
1389 neuroimage.2018.05.027 1431
- 1390 1432
- 1391 1433
- 1392 1434
- 1393 1435
- 1394 1436
- 1395 1437
- 1396 1438
- 1397 1439
- 1398 1440
- 1399 1441
- 1400 1442
- 1401 1443
- 1402 1444
- 1403 1445
- 1404 1446
- 1405 1447
- 1406 1448
- 1407 1449
- 1408 1450
- 1409 1451
- 1410 1452
- 1411 1453
- 1412 1454
- 1413 1455
- 1414 1456
- 1415 1457
- 1416 1458
- 1417 1459
- 1418 1460
- 1419 1461
- 1420 1462
- 1421 1463
- 1422 1464
- 1423 1465
- 1424 1466
- 1425 1467
- 1426 1468
- 1427 1469
- 1428 1470
- 1429 1471
- 1430 1472
- 1431 1473
- 1432 1474
- 1433 1475
- 1434 1476
- 1435 1477
- 1436 1478
- 1437 1479
- 1438 1480
- 1439 1481
- 1440 1482
- 1441 1483
- 1442 1484
- 1443 1485
- 1444 1486
- 1445 1487
- 1446 1488
- 1447 1489
- 1448 1490
- 1449 1491
- 1450 1492
- 1451 1493
- 1452 1494
- 1453 1495
- 1454 1496
- 1455 1497
- 1456 1498
- 1457 1499
- 1458 1500
- 1459 1501
- 1460 1502
- 1461 1503
- 1462 1504
- 1463 1505
- 1464 1506
- 1465 1507
- 1466 1508
- 1467 1509
- 1468 1510
- 1469 1511
- 1470 1512
- 1471 1513
- 1472 1514
- 1473 1515
- 1474 1516
- 1475 1517
- 1476 1518
- 1477 1519
- 1478 1520
- 1479 1521
- 1480 1522
- 1481 1523
- 1482 1524
- 1483 1525
- 1484 1526
- 1485 1527
- 1486 1528
- 1487 1529
- 1488 1530
- 1489 1531
- 1490 1532
- 1491 1533
- 1492 1534
- 1493 1535
- 1494 1536
- 1495 1537
- 1496 1538
- 1497 1539
- 1498 1540
- 1499 1541
- 1500 1542

Conflict of Interest Statement: The authors declare that the research was conducted in the absence of any commercial or financial relationships that could be construed as a potential conflict of interest.

Copyright © 2019 Maffei, Sarubbo and Jovicich. This is an open-access article distributed under the terms of the Creative Commons Attribution License (CC BY). The use, distribution or reproduction in other forums is permitted, provided the original author(s) and the copyright owner(s) are credited and that the original publication in this journal is cited, in accordance with accepted academic practice. No use, distribution or reproduction is permitted which does not comply with these terms.